MRS Advances © 2016 Materials Research Society
DOI: 10.1557/adv.2016.667

Comparison of Capacity Retention Rates During Cycling of Quinone-Bromide Flow Batteries

Michael R. Gerhardt[1], Eugene S. Beh[1,2], Liuchuan Tong[2], Roy G. Gordon[1,2], and Michael J. Aziz[1]

[1]Harvard John A. Paulson School of Engineering and Applied Sciences, Cambridge, MA 02138, U.S.A.
[2]Department of Chemistry and Chemical Biology, Harvard University, Cambridge, MA 02138, U.S.A.

ABSTRACT

We use cyclic charge-discharge experiments to evaluate the capacity retention rates of two quinone-bromide flow batteries (QBFBs). These aqueous QBFBs use a negative electrolyte containing either anthraquinone-2,7-disulfonic acid (AQDS) or anthraquinone-2-sulfonic acid (AQS) dissolved in sulfuric acid, and a positive electrolyte containing bromine and hydrobromic acid. We find that the AQS cell exhibits a significantly lower capacity retention rate than the AQDS cell. The observed AQS capacity fade is corroborated by NMR evidence that suggests the formation of hydroxylated products in the electrolyte in place of AQS. We further cycle the AQDS cell and observe a capacity fade rate extrapolating to 30% loss of active species after 5000 cycles. After about 180 cycles, bromine crossover leads to sufficient electrolyte imbalance to accelerate the capacity fade rate, indicating that the actual realization of long cycle life will require bromine rebalancing or a membrane less permeable than Nafion® to molecular bromine.

INTRODUCTION

Cost effective grid scale energy storage would enable large-scale decarbonization of our electric grid. Redox flow batteries (RFBs) are a potentially low-cost solution to the intermittency problem faced by renewable energy sources such as wind and solar, but their viability requires long cycle life as well as long calendar life [1].

Recently, quinones have been demonstrated as inexpensive electroactive species for aqueous flow batteries [2-5]. One hundred charge-discharge cycles have been demonstrated in an all-quinone flow battery using a tiron posolyte (positive electrolyte) and an anthraquinone-2,6-disulfonic acid negolyte (negative electrolyte), at 35% depth of discharge, with no mention of capacity retention [5]. Our group demonstrated 750 deep cycles of a quinone-bromide flow battery (QBFB) using anthraquinone-2,7-disulfonic acid (AQDS, figure 1a), with 99.84% capacity retention per cycle [6].

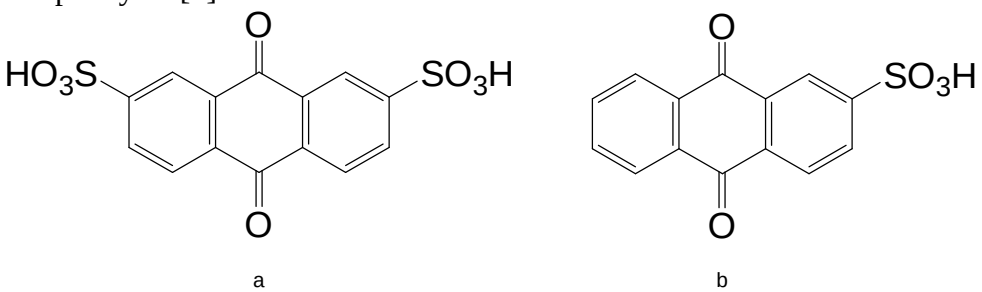

Figure 1. The structures of **a.** AQDS and **b.** AQS.

The AQDS-bromine battery voltage could be increased by using anthraquinone-2-sulfonic acid (AQS, figure 1b) as the negative electrolyte in place of AQDS, because AQS has a lower reduction potential than AQDS. In this work, we examine the long term stability of AQS and AQDS electrolytes in QBFBs through full-cell cycling and chemical analysis. Additionally, we surpass our previous capacity retention rate metric and achieve the highest capacity retention rate reported to date for a quinone-bromide flow battery, extrapolating to 30% loss of active species after 5000 operating cycles.

EXPERIMENT

All electrochemical experiments were performed with a Gamry Reference 3000 potentiostat. Full-cell cycling experiments were performed with an additional Gamry Reference 30k booster**.** The flow cell, including a Nafion® 212 membrane, is described in Ref [7]. Three sheets of Sigracet 10-AA carbon paper (SGL Group), cut to 5 cm^2 and baked in air at 400 °C for 24 hours, were used as electrodes on each side of the membrane. AQDS and AQS electrolytes were prepared via an ion exchange process [2] to yield the acid form.

AQDS and AQS cycling

The cycling performance of AQS and AQDS cells was compared by constant current charge/discharge cycles at two different current densities. The cell was assembled with 25 mL of 1 M AQDS, 1 M H_2SO_4 negolyte and 100 mL of 3 M HBr, 0.5 M Br_2, and 0.5 M H_2SO_4 posolyte. H_2SO_4 was added to the posolyte to improve the osmotic balance between the two electrolytes. The cell was cycled 30 times at 0.25 A/cm^2, 10 times at 0.1 A/cm^2, and 50 additional times at 0.25 A/cm^2, with voltage cutoffs at 1.3 V and 0.3 V. Without disassembling the cell, both sides were flushed with DI water, the AQDS negolyte was replaced with an AQS negolyte (1 M, in 2 M H_2SO_4 to keep the total free[1] proton concentration at 3 M), and the posolyte was replaced with a freshly prepared solution of 3 M HBr, 0.5 M Br_2, and 0.5 M H_2SO_4. Following the same set of 90 cycles, the AQS electrolyte was replaced with fresh AQDS electrolyte to investigate possible aging effects, and the posolyte replaced as before.

Evaluation of quinone crossover via cyclic voltammetry

To evaluate quinone crossover via cyclic voltammetry, 2 mL samples of each posolyte solution were taken after the 90-cycle experiment. Each sample was heated at 70 °C overnight to evaporate bromine. Following heating, each sample was re-dissolved in 20 mL of 1 M H_2SO_4. Cyclic voltammograms were performed with a 3 mm diameter glassy carbon working electrode (polished with 50 nm alumina slurry); an Ag/AgCl reference electrode (3 M NaCl filling solution, BASi); and a Pt coil counter electrode.

Chemical analysis of negolytes before and after cycling

^{1}H NMR spectra were recorded on Varian INOVA 500 spectrometers and are reported in parts per million (ppm). Each sample solution a – d consisted of a 20 µL aliquot of a negolyte prepared as described above (see: AQDS and AQS cycling), first diluted to 20 mL with 1 M H_2SO_4. Subsequently, a 10.0 µL aliquot of each of these solutions was further diluted to 1.00 mL

[1] The pK_a for the second deprotonation of sulfuric acid is 1.99. Therefore, at these solution pH values (~ pH 0), sulfuric acid is predominantly only singly deprotonated as H^+ and HSO_4^-.

http://dx.doi.org/10.1557/adv.2016.667

with the same stock solution of 10.0 mM sodium methanesulfonate in deuterium oxide (D_2O). The sodium methanesulfonate functions as an internal standard, allowing the relative amounts of each substance to be quantified. Samples a and b were produced from the first AQDS negolyte before and after the 90 cycle experiment respectively. Samples c and d were produced from the AQS negolyte before and after the 90 cycle experiment respectively. In order to correct for the different NMR sensitivity of each proton, a very long relaxation time (*d1* = 10.0 s) was utilized.

High-resolution LC-MS analyses of the cycled AQDS and AQS negolytes were performed in the Small Molecule Mass Spectrometry Facility at Harvard University using Agilent ESI-TOF with HPLC.

High capacity retention and posolyte-limit experiments

The cell was assembled as described above, with the exception of the use of custom-built pyro-sealed interdigitated flow plates from Entegris. The flow plates are identical to the previous plates, with the exception of the milled surfaces of the channels being sealed in the Entegris plates. The sealing of the flow channels prevents seepage of fluid into the pores in the graphite. The negolyte was 20 mL of 1 M AQDS in 1 M H_2SO_4, and the posolyte was 120 mL of 0.5 M Br_2 in 3 M HBr. The cell was cycled at 0.25 A/cm^2 with voltage cutoffs of 1.3 V and 0.3 V.

RESULTS AND DISCUSSION

Capacity retention in AQDS-Br and AQS-Br cells

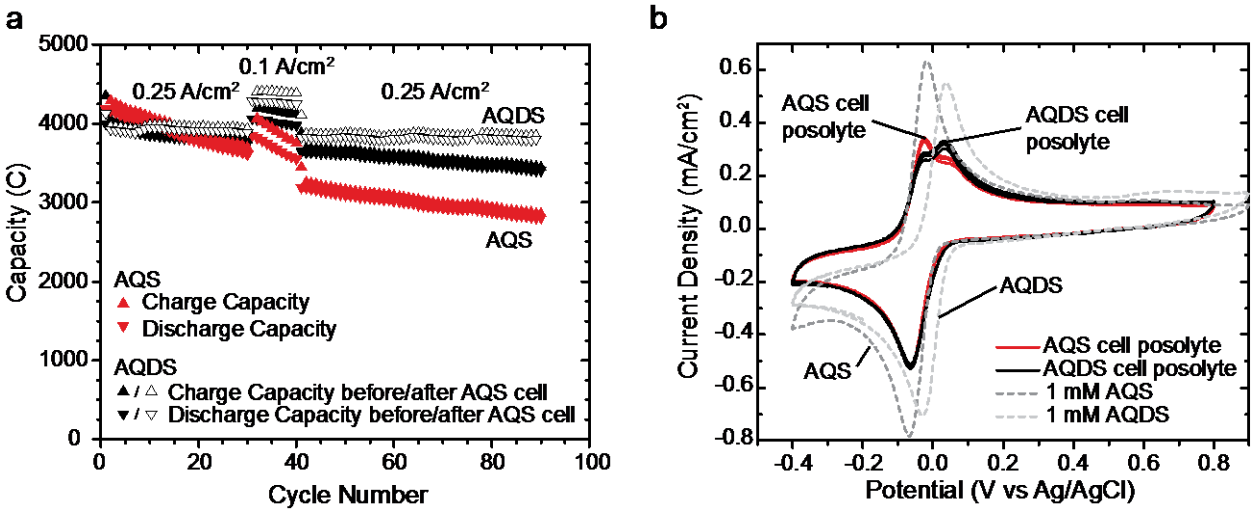

Figure 2. a. Charge and discharge capacities for AQS-bromide and AQDS-bromide cells. All three experiments were performed successively with the same cell build, by flushing the cell and replacing the electrolytes. First, an AQDS negolyte was cycled against a Br_2/HBr posolyte (solid black triangles). Second, an AQS negolyte was cycled against a fresh posolyte (solid red triangles). Third, a fresh AQDS negolyte was cycled against a third fresh posolyte (open black triangles). **b.** Cyclic voltammograms of the posolyte from the AQS-Br cell (red) and the second AQDS-Br cell (black); in each case, the posolyte was first heated to evaporate Br_2. For comparison, we show pristine 1 mM AQS and 1 mM AQDS (dashed lines) in 1 M H_2SO_4.

As can be seen in Figures 2 and 3, the capacity of the AQS cell drops more rapidly than that of the AQDS cell. The capacity retention rate is also dependent on cycling time, which suggests a time-dependent loss mechanism causing more loss over the longer 0.1 A/cm^2 cycles.

Due to a large excess of bromine and hydrobromic acid, the negolyte in these cells is the capacity-limiting electrolyte. For these cells, we suspect that the mechanisms causing capacity loss are dilution of the negolyte, negolyte leakage, and crossover and decomposition of negolyte active species [3].

Table 1. Volume of the negolyte during cycling for each of the three cell cycling runs.

	AQDS (Before AQS)	AQS	AQDS (After AQS)
Volume Gain (mL)	8 ± 1	12 ± 1	13 ± 1
Final Volume (mL)	33 ± 1	37 ± 1	38 ± 1

Dilution of the negolyte, which can be caused by osmotic imbalance between the electrolytes and electroosmotic drag, has an indirect effect on the observable cell capacity as it can increase the mass transport overpotential within the porous electrode, causing the cell to reach the voltage limits sooner than expected. Negolyte dilution was observed during cycling by using a graduated cylinder as the negolyte reservoir. The volume gain was approximately the same for the AQS and AQDS cell runs over time, as shown in Table 1, indicating that negolyte dilution cannot explain the observed difference in capacity retention between AQS and AQDS cells. The volume measurements also rule out negolyte leakage as a potential explanation for the capacity retention difference.

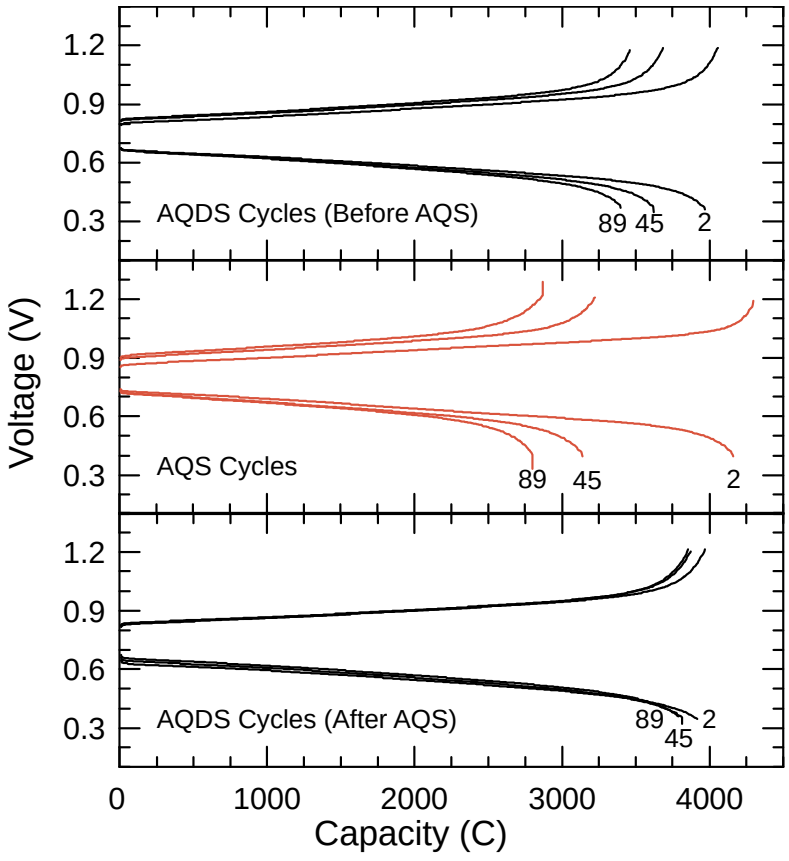

Figure 3. Examples of voltage traces obtained from constant current cycling.

http://dx.doi.org/10.1557/adv.2016.667

Crossover of AQDS and AQS

To further investigate the crossover rates of the quinones, the cycled electrolytes were analyzed via cyclic voltammetry (Figure 2b) to quantify the posolyte quinone contents in each case. The bulk concentration C^* of an electroactive species can be estimated from the peak current density i_p of a cyclic voltammogram if the diffusivity D and number of electrons transferred n are known via the Randles-Sevcik equation [8]:

$$i_p = 0.4463\left(\frac{F^3}{RT}\right)n^{3/2}D^{1/2}C^*\nu^{1/2} \quad (1),$$

in which F represents Faraday's constant (96,485 C/mol), R the universal gas constant (8.314 J/mol K) and T the temperature of the solution (taken to be 298 K). The diffusivity of AQDS was measured [2] to be 3.8(1) × 10^{-6} cm^2/s, whereas for AQS [4] it is 3.71 × 10^{-6} cm^2/s. Assuming n = 2, with the scan rate ν set to 100 mV/s, the reduction peak of quinones suggests a concentration of 7 mM quinone in the posolyte in each case, indicating approximately 135 C (~3.5%) of lost capacity. This measured quinone crossover is equivalent to a capacity loss current of 0.04 mA/cm^2. The similarity in the reduction peak height between each sample indicates approximately equal concentrations of AQDS and AQS that have crossed over to each posolyte. Alternatively, this result could indicate trace amounts of AQS or AQDS remaining in the posolyte after flushing. Therefore, this experiment sets an upper bound on the amount of AQDS and AQS crossover that occurred. Because this upper limit still fails to account for all the capacity lost, we cannot ascribe the reduced capacity retention in AQS cells to crossover.

Possible decomposition of AQS

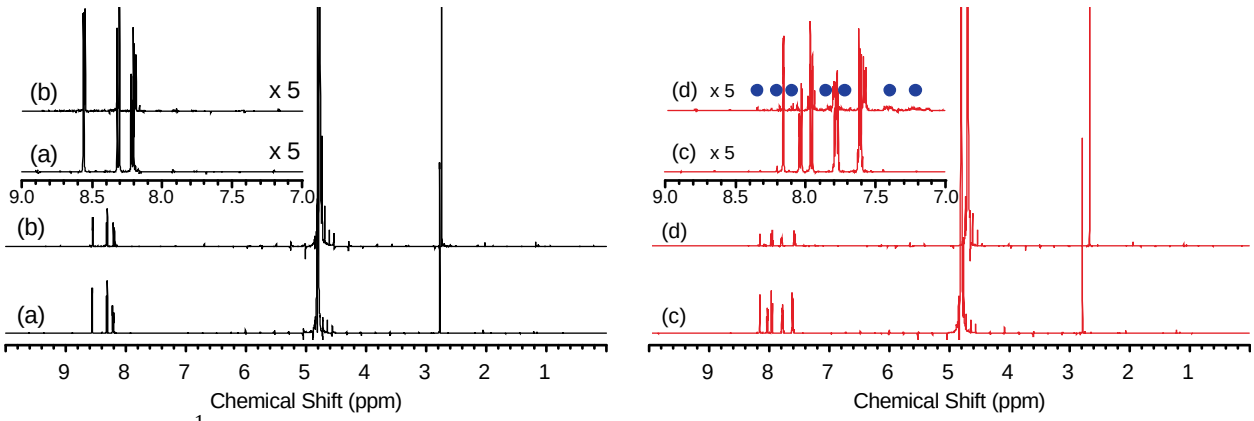

Figure 4. a-b. ^1H NMR spectra of AQDS before (a) and after (b) cycling against aqueous $HBr/Br_2/H_2SO_4$ for 90 cycles. **c-d.** NMR spectra of AQS before (c) and after (d) cycling against aqueous $HBr/Br_2/H_2SO_4$ for 90 cycles. Peaks at ~4.8 ppm and ~2.8 ppm correspond to partially deuterated water (HDO) and sodium methanesulfonate respectively, the latter of which was added as an internal integration standard. Spectra heights are normalized to the area under each peak at ~2.8 ppm. Inset: Magnification (x5) of the 7.0 – 9.0 ppm region. Cycling of AQS is associated with the formation of other NMR-active organic compounds that appear further upfield compared to AQS (peaks marked); for AQDS no NMR-active decomposition products could be identified.

http://dx.doi.org/10.1557/adv.2016.667

Each electrolyte was examined before and after cycling by NMR (Figure 4). In either case loss of the starting material could be observed as a decrease in peak area: for AQS, 33% of the AQS peak area remained after cycling, whereas for AQDS, 58% remained. After correcting for negolyte dilution (Table 1), these results indicate 52% moles AQS remaining and 76% moles AQDS remaining in their respective negolytes.

The appearance of new peaks in the AQS NMR spectrum indicates a decomposition product or products. From the upfield chemical shift of the AQS decomposition products, it appears that one or more aromatic protons on AQS is substituted with an electron-donating group, likely -OH. The integration for the decomposition products, however, does not account for all the AQS lost, so this material likely ends up decomposing further into either an insoluble product, or a product containing no C-H bonds. High-resolution mass spectrometry on the cycled AQS negolyte revealed the existence of 2-hydroxy-9,10-anthraquinone (m/z = 272.0149 ± 0.005), suggesting the replacement of a sulfonate with a hydroxy group during cycling, resulting in an insoluble compound.

Although the concentration of AQDS before and after cycling appears to have dropped, no decomposition products were detectable by NMR. One possibility is that AQDS decomposes into numerous different products, each of which is too small in quantity to detect. Alternatively, AQDS could decompose into an insoluble or NMR-inactive species, or a species that interacts with bromine to form an insoluble or NMR-inactive species. High-resolution mass spectrometry on the cycled negolyte revealed three additional compounds, with masses suggesting (1) the replacement of one sulfonate with a hydroxy group (m/z = 302.9963 ± 0.005), (2) the replacement of both sulfonates with hydroxy (m/z = 239.0344 ± 0.005), and (3) the addition of a hydroxy without replacing a sulfonate (m/z = 382.9532 ± 0.005). Compounds (1) and (3) are likely to remain soluble and electrochemically active, so their formation may not result in capacity fade.

Both AQDS and AQS in their oxidized forms appear to be stable, even in boiling Br_2 and HBr [2, 7]. Hence we believe these reactions to start with the reduced forms of AQDS and AQS.

Extending AQDS-Br cycle life & impact of bromine crossover on cycle life

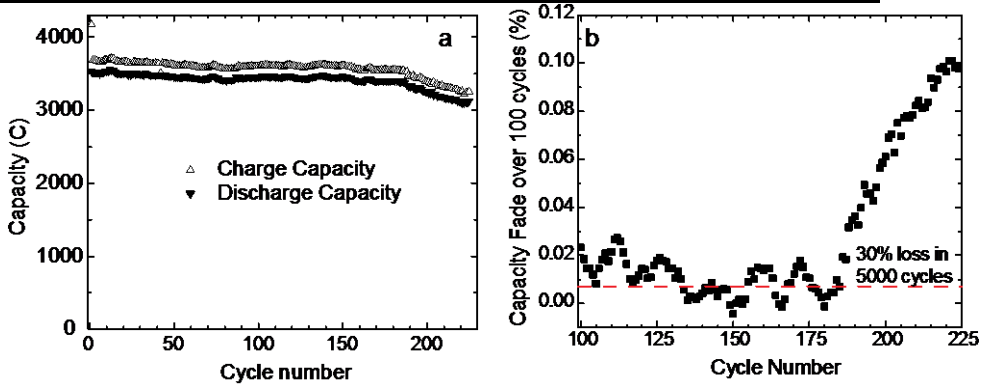

Figure 5. a. Charge and discharge capacities and **b.** capacity fade over prior 100 cycles as a function of cycle number in an AQDS-bromide cell.

To further examine the long-term stability of AQDS, an AQDS-bromide cell was constructed and cycled at 0.25 A/cm^2 for over 200 cycles. The cell shows excellent capacity retention initially, before a rapid drop in capacity near cycle 183, as shown in Figure 5a. Figure 5b reports the capacity fade per 100 cycles, for each set of continuous 100 cycles in the 225

cycle experiment. The dashed line represents the fade rate (0.00713% per cycle) that extrapolates to 70% remaining capacity after 5000 cycles. Thus, after an initial conditioning period, the cell is able to cycle with this capacity fade rate — with some noise — until the sudden increase in capacity fade. Converted to a capacity loss current (0.03 mA/cm^2), this low capacity fade rate is approximately equivalent to our measurements of quinone crossover rates (see: Crossover of AQDS and AQS), indicating that this capacity loss is likely due to AQDS crossover.

We attribute the sudden increase in cycle fade at cycle 183 to a change in the capacity-limiting electrolyte of the cell. The current efficiency averaged 95.7%. Thus, the state of charge of the posolyte gradually increases as the cell is cycled, because 4.3% of the bromine produced during each charge cycle is not converted back to bromide. Once there is insufficient bromide, bromide in the posolyte becomes the capacity-limiting reagent in the cell upon charging, at which point the capacity begins its rapid decline [3]. Converted to a capacity loss current, this new fade rate (0.23 mA/cm^2) is less than what would be predicted by bromine crossover alone (1.2 mA/cm^2) [3]. This discrepancy could be due to variation in bromine crossover rate with posolyte state of charge[9].

CONCLUSIONS

The AQS-bromine cell exhibits a lower capacity retention rate than does the AQDS-bromine cell. AQS appears to undergo a hydroxylation/decomposition reaction. With careful control of AQDS leakage from the cell by sealing the flow plate channels, an AQDS-bromide flow battery can be cycled hundreds of times with high capacity retention. The extrapolation to 30% capacity loss in 5000 cycles is interrupted by the onset of a sudden capacity fade mechanism which we interpret as the posolyte becoming the capacity-limiting side. This result indicates that AQDS will survive 5000 reductions and 5000 oxidations without unacceptable amounts of molecule destruction, assuming sufficient posolyte supply.

Presently, loss of bromine from the posolyte limits the lifetime of the AQDS-bromide flow battery. The development of bromine rebalancing methods, bromine complexing agents, or membranes impermeable to bromine appears to be critical for long-term operation of aqueous-soluble organic flow batteries containing bromine.

ACKNOWLEDGMENTS

This work was partially funded through the US Department of Energy ARPA-E Award #DE-AR0000348 and partially funded through the Harvard John A. Paulson School of Engineering and Applied Sciences. This work was also supported by funding from the Massachusetts Clean Energy Technology Center. We acknowledge Sergio Granados-Focil, Marc-Antoni Goulet, David Kwabi, and Andrew Wong for helpful discussions and a critical reading of the manuscript.

REFERENCES

1. G. L. Soloveichik, Chem Rev **115** (20), 11533-11558 (2015).
2. B. Huskinson, M. P. Marshak, C. Suh, S. Er, M. R. Gerhardt, C. J. Galvin, X. Chen, A. Aspuru-Guzik, R. G. Gordon and M. J. Aziz, Nature **505** (7482), 195-198 (2014).
3. Q. Chen, L. Eisenach and M. J. Aziz, Journal of The Electrochemical Society **163**, A5057-A5063 (2016).

4. B. Yang, L. Hoober-Burkhardt, F. Wang, G. K. Surya Prakash and S. R. Narayanan, Journal of the Electrochemical Society **161**, A1371-A1380 (2014).
5. B. Yang, L. Hoober-Burkhardt, S. Krishnamoorthy, A. Murali, G. K. S. Prakash and S. R. Narayanan, Journal of The Electrochemical Society **163** (7), A1442-A1449 (2016).
6. B. Huskinson, M. P. Marshak, M. R. Gerhardt and M. J. Aziz, ECS Transactions **61**, 27-30 (2014).
7. M. R. Gerhardt, L. Tong, R. Gómez-Bombarelli, Q. Chen, M. P. Marshak, C. J. Galvin, A. Aspuru-Guzik, R. G. Gordon and M. J. Aziz, Advanced Energy Materials, 1601488 (2016).
8. A. J. Bard and L. R. Faulkner, *Electrochemical methods : fundamentals and applications*. (Wiley, New York, 2001).
9. K. T. Cho, M. C. Tucker, M. Ding, P. Ridgway, V. S. Battaglia, V. Srinivasan and A. Z. Weber, ChemPlusChem **80** (2), 402-411 (2015).

http://dx.doi.org/10.1557/adv.2016.667